

Design of photonic crystal fiber long-period grating refractive index sensor

Jiri Kanka^{*a}, Yinian Zhu^b, Zonghu He^b and Henry Du^b

^aInstitute of Photonics and Electronics, Academy of Science of the Czech Republic,
Chaberska 57, 182 51 Prague, Czech Republic;

^bDepartment of Chemical Engineering and Materials Science, Castle Point on Hudson,
Hoboken, New Jersey 07030, USA

ABSTRACT

Numerical optimization of photonic crystal fiber (PCF) structures for refractive index sensors based on long period gratings inscribed in PCFs has been performed. The optimization procedure employs the Nelder-Mead downhill simplex algorithm. This direct-search method attempts to minimize a scalar-valued nonlinear function of N real variables (called the objective function) using only function values, without any derivative information. An inverse design approach utilizes the objective function constructed using desired sensing characteristics. For the modal analysis of the PCF structure a fully-vectorial solver based on the finite element method is called by the objective function. The dispersion optimization of PCFs is aimed at achieving a high sensitivity of measurement of refractive index of analytes infiltrated into the air holes for the refractive index and probe wavelength ranges of interest. We have restricted our work to the index-guiding solid-core PCF structures with hexagonally arrayed air holes.

Keywords: Photonic crystal fibers, fiber design, long-period gratings, refractive index sensors, finite element method, simplex downhill method

1. INTRODUCTION

In recent years, long period gratings (LPGs) have been intensively studied for applications in the telecommunications and fiber optic sensing fields. LPG devices have been developed as gain-flattening devices for erbium-doped fibre amplifiers, band rejection filters¹ and temperature, strain, refractive index and bend sensors.²⁻⁴

In general, an LPG may be created by introducing a periodic refractive index modulation in the fiber core by exposing it to intense modulated ultraviolet radiation that is absorbed by the fiber. In the LPG, the incident core mode is coupled resonantly to a cladding mode by a periodic perturbation that equals the beat length between the two modes. Phase matching between the mode propagating in the core of the fibre and a forward-propagating cladding mode is achieved at the wavelength, λ , where the expression

$$\lambda = [n_{co}(\lambda) - n_{cl}(\lambda)]\Lambda_G, \quad (1)$$

is satisfied,¹ where n_{co} and n_{cl} are the effective refractive indices of the propagating core mode and cladding mode at wavelength λ , respectively and Λ_G is the periodicity of the LPG.

In standard optical fibers the cladding mode probes the surroundings of the fiber, and in this way the resonance wavelength may be shifted. The shift in resonance wavelength is used as the indicator of the refractometer.⁵ LPGs can also be realized in photonic-crystal fibers (PCFs).⁶ These fibers consist of an array of air holes running along the fiber axis. The holes in the cladding are most commonly placed in a periodic triangular structure, which is characterized by a lattice constant (pitch), Λ , and the diameter of the holes, d . We consider index guiding PCFs, which have a solid core in the form of a missing air hole in the center. In index guiding PCFs light is confined to the core by modified total internal reflection, analogous to guiding in standard optical fibers. The hole structure in the cladding determines the optical properties of the PCF, which allows for a large degree

*kanka@ufe.cz, phone: 00 420 266 773 526

of freedom in tailoring the PCF properties through control of the hole size and pitch. The propagating wave inside the PCF can have a particularly strong evanescent wave compared with a standard optical fiber owing to a much-closer proximity of the electromagnetic wave and the holes than the exterior of the fiber. The air holes of the PCF provide access for the sample to the regions with a strong evanescent wave. The probing of holes is stronger for a small pitch and for large air holes.⁷

Recent research of the dispersion property of long-period fiber gratings in an conventional B/Ge codoped fiber^{8,9} has shown that high-order modes have interesting waveguide-dispersion characteristics. It was estimated theoretically that each mode has a 'dispersion turning point' at which $d\lambda/d\Lambda_G \rightarrow \infty$ and in or around that point, it exhibits the highest sensitivity to external parameters. Therefore an LPG with a particular period can be designed accordingly to show the highest sensitivity available by selecting that mode which exhibits a turning point in the phase matching curve. Moreover, there is the dual resonance exhibited by a coupled cladding mode with a phase-matching condition that is close to the dispersion-turning point, which has been exploited for refractive-index sensing.^{10,11}

The lowest-order cladding mode, designated here as the LP₀₂ cladding mode (it is similar to the LP₀₂ mode of the step-index fiber), was selected for resonant coupling with the LP₀₁ core mode.¹² The LP₀₁ and LP₀₂ modes have the largest field overlap and the same symmetry and linear polarization, which maximizes their coupling strength (see Figs. 1 and 2).

In this work, using an inverse design,^{13,14} we have tried to optimize mode dispersion properties and refractive index sensitivity of PCF-LPG structures. Employing the Nelder-Mead simplex method¹⁵ we will be seeking an optimal pitch and diameter of air holes to get for LP₀₁-LP₀₂ mode coupling the phase matching curve with the dispersion turning point located in the given ranges of resonant wavelengths and refractive indices of an analyte infiltrated into air holes.

2. INVERSE DESIGN METHOD

In order to calculate the wavelength dependence of the effective index (n_{eff}) of the modes of PCF, we employ a commercial full-vector mode solver based on the Finite Element Method (FEM). Taking into account the symmetry of PCF with hexagonally arrayed air holes and mode classes of the LP₀₁ core mode and LP₀₂ cladding mode we can reduce the computational window to one-quarter of the fiber cross-section with a perfect electric and magnetic conductor boundary condition applied along symmetric planes.¹⁶ In order to further reduce the simulated waveguide cross section and enable us to evaluate the PCF mode's confinement loss, anisotropic perfectly-matched layers¹⁷ are positioned outside the outmost ring of air holes. The confinement loss CL is deduced from the value of n_{eff} as¹⁷

$$\text{CL} = 8.686 \text{ Im} [2\pi/\lambda \cdot n_{\text{eff}}] \quad (2)$$

in dB/m, where Im stands for the imaginary part.

The material dispersion of fused silica glass is directly included in the calculation. The refractive index as a function of wavelength for fused silica is given by the Sellmeier equation

$$n^2 = 1 + \frac{B_1\lambda^2}{\lambda^2 - C_1^2} + \frac{B_2\lambda^2}{\lambda^2 - C_2^2} + \frac{B_3\lambda^2}{\lambda^2 - C_3^2}, \quad (3)$$

where $B_1 = 0.6961663$, $B_2 = 0.4079426$, $B_3 = 0.8974794$, $C_1 = 0.0684043$, $C_2 = 0.1162414$, $C_3 = 9.896161$ and wavelength λ is in μm .¹⁸

For the dispersion optimization we have defined the objective function to be minimized with the Nelder-Mead Simplex Method as

$$F = \sum_{\lambda_i=1.3\mu\text{m}}^{1.7\mu\text{m}} \left| \frac{d\Lambda_G}{d\lambda}(\lambda_i) \right|, \quad (4)$$

where the derivative of Λ_G with respect to λ is calculated at a wavelength λ_i and the sum is performed over 5 (uniformly spaced) points in the interval. The free parameters are the pitch of the triangular lattice, Λ , and

the diameter d_i of the air holes normalized by the pitch Λ . The constraints imposed on the air-hole diameter ($d \geq 2.5 \mu\text{m}$) and air-filling ratio ($d/\Lambda \leq 0.9$) were additionally introduced into the objective function as penalty terms for constraint violation.

3. OPTIMIZED FIBERS AND DISCUSSION

The geometrical parameters of the optimized PCFs for LP₀₁-LP₀₂ mode coupling with the dispersion turning point in the middle of the 1.3 - 1.7 μm range and for given values of the analyte refractive index n are listed in Table 1. Phase matching LPG periodicity, Λ_G , percentage power overlaps with air holes for the LP₀₁ core mode, Overlap01, and LP₀₂ cladding mode, Overlap02, and confinement loss of LP₀₂ mode, CL02, all calculated for a coupling wavelength of 1.5 μm , are also given in Table 1.

Table 1. Geometrical parameters and optical properties (calculated at 1.5 μm) of the optimized fibers.

Fiber	n	Λ [μm]	d_{1-4}/Λ	d_5/Λ	Λ_G [μm]	Overlap01 [%]	Overlap02 [%]	CL02 [dB/m]
F1	1.15	3.431	0.729	0.900	34	0.69	8.7	$8.1 \cdot 10^{-3}$
F2	1.25	4.245	0.736	0.900	51	0.67	8.5	$5.5 \cdot 10^{-3}$
F3	1.33	5.753	0.736	0.900	92	0.60	7.5	$1.6 \cdot 10^{-3}$
F4	1.40	10.154	0.728	0.900	283	0.45	5.6	$1.1 \cdot 10^{-4}$
F5	1.33	5.799	0.740	0.740	91	0.59	7.6	$3.8 \cdot 10^2$

Comparison of Overlap01 and Overlap02 shows more than 12 times higher evanescent wave overlap with an analyte in holes obtained thanks to LP₀₁-LP₀₂ mode coupling in the LPG. Fibers F1, F2, F3 and F4 have been optimized with the ratio d_5/Λ set to 0.9, where d_5 is the diameter of air holes in the 5th ring. By enlarging the air holes in the outmost ring the LP₀₂ cladding mode confinement loss has been reduced to a negligible level. This makes possible a complementary implementation of evanescent PCF-LPG refractive-index sensing with a direct detection of light coupled into the LP₀₂ cladding mode at the PCF output or a scheme with two separated apart LPGs for LP₀₁-LP₀₂ coupling and LP₀₂-LP₀₁ recoupling utilizing a longer interaction length with an analyte. In Fiber F5 with the equal air hole diameters in all rings the LP₀₂ cladding mode confinement loss is about 400 dB/m, which enable us to use a standard LPG sensing based on the measurement of resonant absorption peaks in the LPG transmission spectrum. Comparing Fiber F3 with Fiber F5 we have found that the change of diameter of holes in the 5th ring has a negligible effect on relevant dispersion characteristics.

It is obvious from Table 1 that dispersion characteristics are tuned with increasing the refractive index n by scaling up the PCF structure as the ratio d/Λ remains almost constant and the pitch Λ increases. Plots of phase matching LPG periodicity as a function of resonant wavelength are shown in Figs. 3, 4, 5 and 6 for Fibers F1, F2, F3 and F4, respectively. High sensitivities are demonstrated in the vicinity of dispersion turning points employing a dual resonance. The ratio of the change in refractive index n to corresponding separation of the dual resonant wavelengths [pm] is around $1 \cdot 10^{-8}$ RIU for all four cases. A quality factor, Q , including also the FWHM of the resonance dip has recently been proposed¹⁹ for characterizing LPG sensors and it will be taken into account in our following numerical optimization of PCF-LPG refractive index sensors.

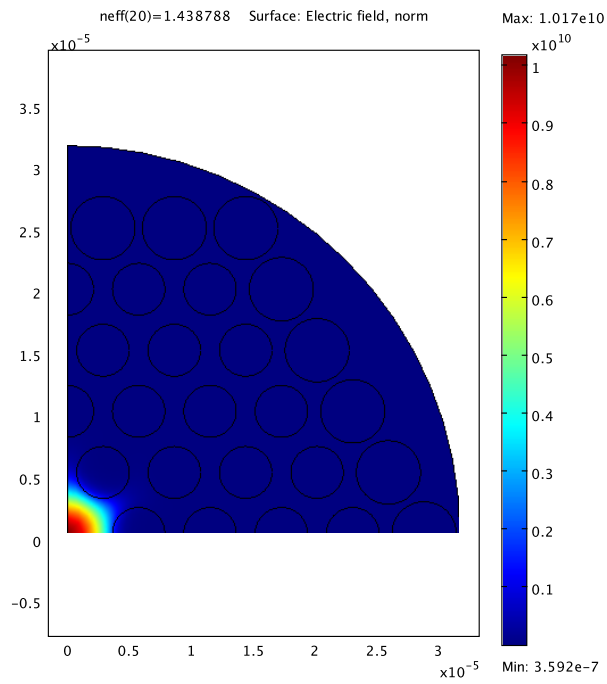


Figure 1. Electric field distribution of LP₀₁ core mode (in Fiber F3 at a wavelength of 1.5 μ m).

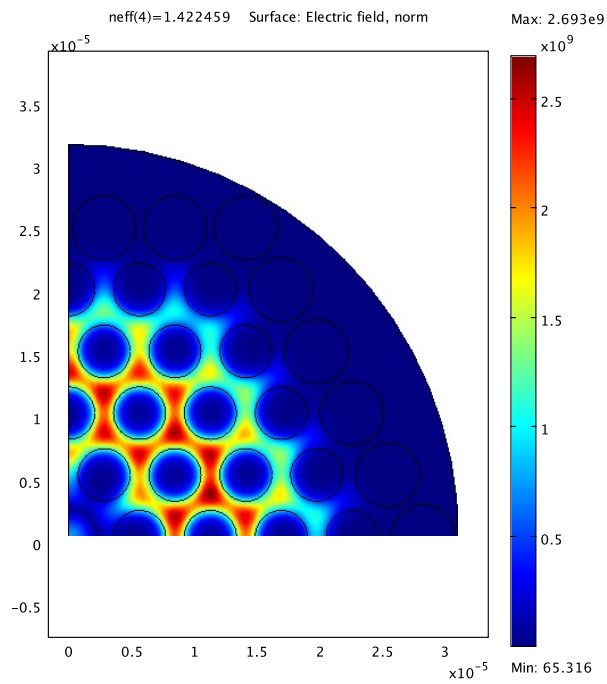


Figure 2. Electric field distribution of LP₀₂ cladding mode (in Fiber F3 at a wavelength of 1.5 μ m).

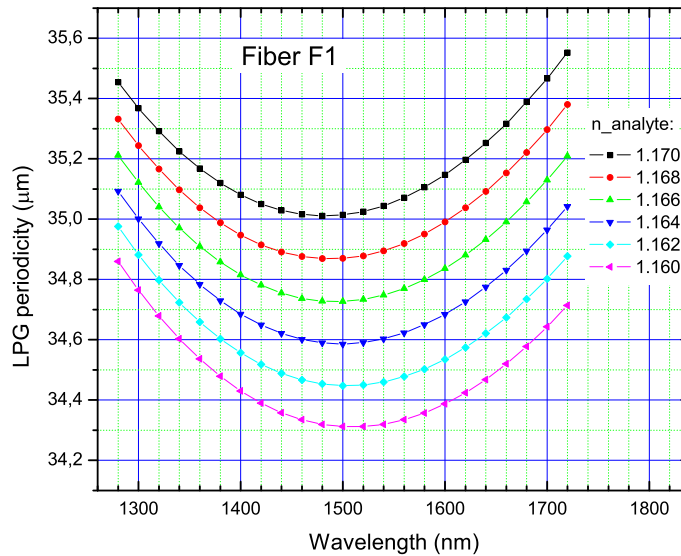


Figure 3. Phase matching LPG periodicity versus the resonant wavelength for PCF optimized for the analyte refractive index of around 1.15 (Fiber F1 in Table 1). For a LPG periodicity of $34.7 \mu\text{m}$ the resonance wavelength at 1500 nm is splitted into two resonant wavelengths which shift in opposite direction to 1380 nm and 1620 nm when the analyte refractive index changes from 1.166 to 1.164.

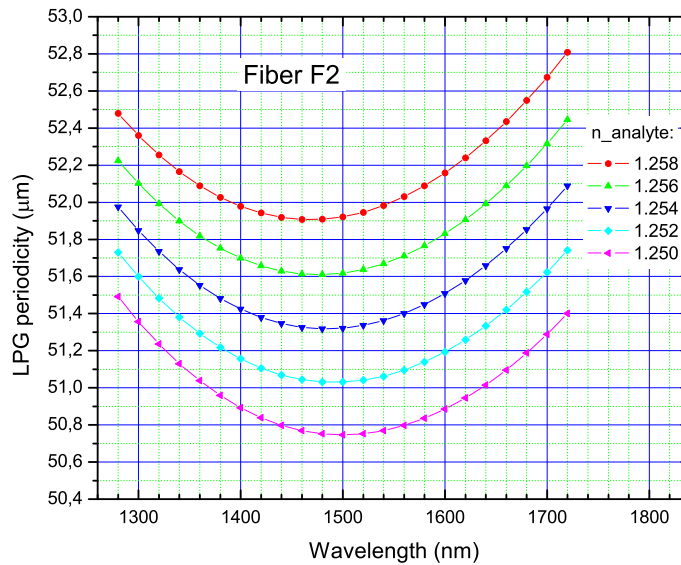


Figure 4. Phase matching LPG periodicity versus the resonant wavelength for PCF optimized for the analyte refractive index of around 1.25 (Fiber F2 in Table 1). For a LPG periodicity of $51.03 \mu\text{m}$ the resonance wavelength at 1500 nm is splitted into two resonant wavelengths which shift in opposite direction to 1360 nm and 1640 nm when the analyte refractive index changes from 1.252 to 1.250.

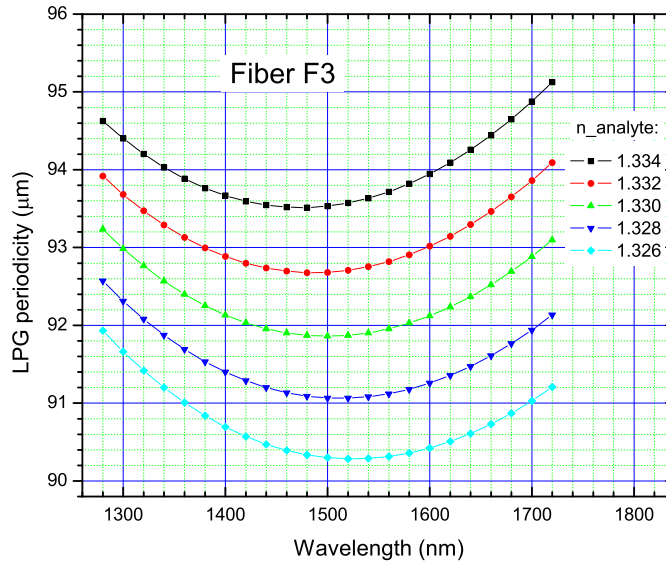


Figure 5. Phase matching LPG periodicity versus the resonant wavelength for PCF optimized for the analyte refractive index of around 1.33 (Fiber F3 in Table 1). For a LPG periodicity of $91.8 \mu\text{m}$ the resonance wavelength at 1500 nm is splitted into two resonant wavelengths which shift in opposite direction to 1340 nm and 1690 nm when the analyte refractive index changes from 1.330 to 1.328.

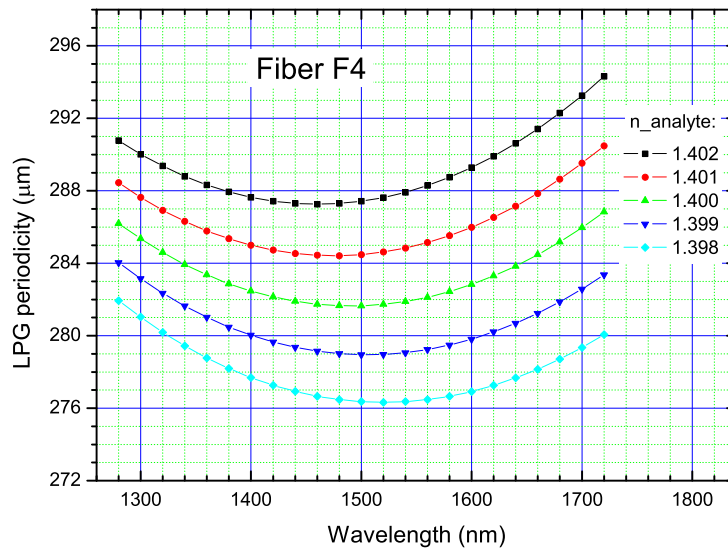


Figure 6. Phase matching LPG periodicity versus the resonant wavelength for PCF optimized for the analyte refractive index of around 1.40 (Fiber F4 in Table 1). For a LPG periodicity of $281.6 \mu\text{m}$ the resonance wavelength at 1500 nm is splitted into two resonant wavelengths which shift in opposite direction to 1340 nm and 1680 nm when the analyte refractive index changes from 1.400 to 1.399.

4. CONCLUSIONS

Using a full-vectorial mode solver based on the finite element method in a combination with the Nelder-Mead simplex method we have performed the dispersion optimization of PCF-LPG structures for refractive index sensing. We have found an optimal pitch and diameter of air holes of PCFs and LPG periodicity to get for LP₀₁ core mode - LP₀₂ cladding mode coupling the phase matching curve with the dispersion turning point located in the given ranges of resonant wavelengths and refractive indices of the analyte infiltrated into air holes. High refractive index sensitivities have been demonstrated in close proximity of dispersion turning points employing the dual resonance. The optimized PCF structures also have an enhanced evanescent wave overlap with the analyte.

ACKNOWLEDGMENTS

This work is partially supported by the Czech Science Foundation under grant number 102-08-1719 and the US National Science Foundation under grant number ECS-0404002.

REFERENCES

- [1] Vengsarkar, A. M., Lemaire, P. J., Judkins, J. B., Bhatia, V., Erdogan, T., and Sipe, J. E., "Long period fiber gratings as band rejection filters," *J. Lightwave Technol.* **14**, 58–64 (1996).
- [2] Bhatia, V., "Applications of long-period gratings to single and multi-parameter sensing," *Opt. Express* **4**, 457–466 (1999).
- [3] James, S. W. and Tatam, R. P., "Optical fibre long-period grating sensors: characteristics and application," *Meas. Sci. Technol.* **14**, R49–R61 (2003).
- [4] Patrick, H., Kersey, A., and Bucholtz, F., "Analysis of the response of long period fiber gratings to external index of refraction," *J. Lightwave Technol.* **16**, 1606–1612 (1998).
- [5] Bhatia, V. and Vengsarkar, A. M., "Optical fiber long-period grating sensors," *Opt. Lett.* **21**, 692–694 (1996).
- [6] Eggleton, B. J., Westbrook, P. S., Windeler, R. S., Spalter, S., and Strasser, T. A., "Grating resonances in air-silica microstructured optical fibers," *Opt. Lett.* **24**, 1460–1462 (1999).
- [7] Fini, J. M., "Microstructure fibres for optical sensing in gases and liquids," *Meas. Sci. Technol.* **15**, 1120–1128 (2004).
- [8] Shu, X., Zhang, L., and Bennion, I., "Sensitivity characteristics near the dispersion turning points of long-period fiber gratings in B/Ge codoped fiber," *Opt. Lett.* **26**, 1755–1757 (2001).
- [9] Shu, X., Zhang, L., and Bennion, I., "Sensitivity characteristics of long-period fiber gratings," *J. Lightwave Technol.* **20**, 255–266 (2002).
- [10] Shu, X., Zhu, X., Jiang, S., Shi, W., and Huang, D., "High sensitivity of dual resonant peaks of long-period fibre grating to surrounding refractive index changes," *Electron. Lett.* **35**, 1580–1581 (1999).
- [11] Chen, X., Zhou, K., Zhang, L., and Bennion, I., "Dual-peak long-period fiber gratings with enhanced refractive index sensitivity by finely tailored mode dispersion that uses the light cladding etching technique," *Appl. Opt.* **46**, 451–455 (2007).
- [12] Zhu, Y., He, Z., Du, H., and Kanka, J., "Numerical analysis of refractive index sensitivity of long-period gratings in photonic crystal fiber," *Sens. Actuator B: Chem.* **129**, 99–105 (2008).
- [13] Poletti, F., Finazzi, V., Monroe, T. M., Broderick, N. G. R., Tse, V., and Richardson, D. J., "Inverse design and fabrication tolerances of ultra-flattened dispersion holey fibers," *Opt. Express* **13**, 3728–3736 (2005).
- [14] Kanka, J., "Design of photonic crystal fibers with highly nonlinear glasses for four-wave-mixing based telecom applications," *Opt. Express* **16**, 20395–20408 (2008).
- [15] Lagarias, J. C., Reeds, J. A., Wright, M. H., and Wright, P. E., "Convergence properties of the Nelder-Mead Simplex Method in low dimensions," *SIAM J. Optim.* **9**, 112–147 (1998).

- [16] Guobin, R., Zhi, W., Shuqin, L., and Shuisheng, J., "Mode classification and degeneracy in photonic crystal fibers," *Opt. Express* **11**, 1310–1321 (2003).
- [17] Saitoh, K., Koshiba, M., Hasegawa, T., and Sasaoka, E., "Chromatic dispersion control in photonic crystal fibers: application to ultra-flattened dispersion," *Opt. Express* **11**, 843–852 (2003).
- [18] Malitson, I. H., "Interspecimen comparison of the refractive index of fused silica," *J. Opt. Soc. Am.* **55**, 1205–1209 (1965).
- [19] Rindorf, L. and Bang, O., "Highly sensitive refractometer with a photonic crystal-fiber long-period grating," *Opt. Lett.* **33**, 563–565 (2008).